



Application of combined cake filtration-intermediate blocking model and intermediate-standard blocking model to ultrafiltration of skim milk

Zahra Amiri Rigi¹, Mansoor Kazemimoghadam²

¹Department of Chemical Engineering, South Tehran Branch, Islamic Azad University, Tehran, Iran

²Malek Ashtar University of Technology, Iran

Abstract

Major drawback in application of ultrafiltration membrane processes is fouling, a complex phenomenon which highly depends on the operational conditions such as pH, temperature, feed velocity, trans-membrane pressure and the geometry of the membrane unit. Milk fouling mostly arises from precipitation of proteins and fats in the form of a cake layer on the surface of the membrane. In this study, combined cake filtration-intermediate blocking model and combined intermediate-standard blocking model were applied to ultrafiltration of skim milk at constant flow rate. The effect of trans-membrane pressure and temperature on flux decline was investigated. Based on the results obtained here, the combined intermediate blocking and standard blocking model provided the best simulation, as it was able to fit the experimental data for skim milk concentration with low error values. With increasing pressure to 100 KPa, the differences between combined cake formation-intermediate blocking model and experimental data increased and with further increase in the pressure the differences decreased.

© 2017 ijrei.com. All rights reserved

Keywords: Ultrafiltration; Fouling; Modeling; Milk Concentration; Combined Models.

1. Introduction

Membrane processes are widely used in food industry, water and wastewater treatment and oil processing due to their improved capacity and also lower energy consumption compared to traditional filtration methods [1-4]. Among them, ultrafiltration membranes are widely applied in dairy industries like milk concentration, cheese making, whey fractionation and milk dehydration processes [5, 6]. Conventional filtration methods are not widely used in dairy industry because of negative impact they have on nutritional properties of the yields. These methods also destroy the natural state of the products, which is associated with the exposure to heat streams and changing the salt and pH content of the feed. Besides that, the high cost of these separation processes as well as their low overall productivity, has made them unsuitable for these purposes [7].

Major drawback in application of ultrafiltration membrane processes is fouling, a complex phenomenon arisen from the accumulation of solutes near the membrane surface and pore entrance, which highly depends on the operational conditions such as pH, temperature, feed velocity, trans-membrane pressure (TMP) and the geometry of the membrane unit [8-10].

Fouling decreases the efficiency of the separation process, declining the flux far below the theoretical capacity of the membrane. To overcome the problem, accurate models are required to predict the flux decline at various operational conditions, in order to consider suitable cleaning process for removal of fouling layer.

There are four mechanisms which are mainly responsible for the fouling, including complete blocking mechanism, intermediate blocking mechanism, cake formation mechanism and standard blocking mechanism [3]. According to intermediate or complete pore blocking models the available membrane area decreases with volume filtered. This decrease in membrane area is associated with the blockage of the membrane's pores with feed solutes. These two models are similar to each other, but the assumption behind the complete blocking model is more severe than the intermediate blocking model. According to the complete blocking model, the particles seal off the pores without superimposition on each other. However, the intermediate blocking model alleviate complete blocking mechanism assumption by assuming that a portion of the solutes block pores and the others superimpose

one another. Standard blocking model assumes that small particles deposit on the inner wall of the membrane's pores, deteriorating the membrane structure and adding additional resistance to feed flow. This fouling mechanism is considered the most severe fouling which cannot be removed by usual cleaning processes. Cake formation model assumes that particles accumulate on the surface of the membrane in the form of a permeable cake layer, adding another resistance to flow [11].

So far, many studies have been carried out to simulate flux decline in ultrafiltration membranes using numerical or mathematical methods. Katsoufidou et al. [12] studied the flux decline during ultrafiltration of humic acid solutions and developed a model which accounted for the simultaneous action of all fouling mechanisms and found that this model fitted the experimental data. Razavi et al. [10] have proposed a model by artificial neural network (ANNs) in ultrafiltration of skim milk which reported results were in good agreement with experimental data. However, the major limitation of ANNs is the need of large experimental data which in many cases is not available. Moreover, obtained model is not comprehensive and cannot be used for other systems.

Mattaraj et al. [13] developed a new combined model to mimic fouling of NOM solutions in nanofiltration membranes, taking pore blocking, osmotic pressure and cake formation into account. Their findings showed different flux decline behaviors in NOM solutions containing sparingly soluble inorganic salts and soluble inorganic salts. The authors found that phosphate species sealed off entrance pores and were the major fouling material. Corbaton-Baguena et al. [14] fitted an exponential model to data for the fouling of polyethylene glycol aqueous, taking concentration polarization, particle accumulation on the surface of the membrane and long-term fouling into account, and found that this model gave accurate predictions of the fouling in severe operational conditions. Briao and Tavares [15] found that the data for the fouling of the dairy wastewater in tubular ultrafiltration membrane could be fitted initially by the complete blocking and subsequently by the cake formation mechanism. They also found that the cake filtration mechanism was the main mechanism responsible for fouling in spiral wound membranes.

Ho and Zydney [16] developed a mathematical model for flux decline during the filtration of bovine serum albumin solution, which accounted for initial fouling due to complete blocking mechanism and subsequently by the cake filtration mechanism. Their proposed mathematical model, which explicitly accounted for the inhomogeneity in the cake layer due to the complete blocking mechanism, was the first model accounted for the combined effects of fouling mechanisms and was in good agreement with the empirical data.

Following Ho and Zydney modeling work, a method was used to develop combined models of fouling with two fitted parameters [3]. The method was to insert explicit equations of resistance and available membrane area as a function of time or volume filtered into Darcy's equation. The equations then were integrated to derive explicit equations of volume filtered

as a function of time in constant pressure operation, or pressure as a function of time in constant flow operation. The two fouling mechanisms were assumed to occur simultaneously. Based on this method five models were developed that accounted for the combined effects of cake filtration-complete blocking, cake filtration-intermediate blocking, complete-standard blocking, intermediate-standard blocking and cake filtration-standard blocking. The models then were compared with experimental data during microfiltration and ultrafiltration of bovine serum albumin and human IgG. The authors found that these models provided better predictions of flux decline compared to individual fouling mechanisms. Their findings also showed that combined cake filtration-complete blocking model provided the best data fits for fouling of biological fluids.

In this study, previous proposed combined cake filtration-intermediate blocking model was compared with combined intermediate-standard blocking model and used to analyze the flux decline during skim milk concentration. The goal was to compare these models with experimental data, to see which of them can best fit the data sets for the ultrafiltration of skim milk. These models were assessed through two different sets of experiments. In the first experiment, ultrafiltration testing under constant temperature and flow rate operation was carried out with reconstituted skim milk solution as feed flow. Reconstituted skim milk was pumped through polysulfone amide ultrafiltration system. The effect of varying trans-membrane pressures on flux was studied. In the second experiment, the ultrafiltration of partially skimmed milk with a Pellicon cassette module was carried out and the effect of temperature and TMP on flux decline was investigated. Based on the results obtained here, the combined standard-intermediate blocking model provided the best fit of the data sets. Therefore, this model can be an effective model for filtration systems where the flux decreases in a manner between the extremes of standard blocking and intermediate blocking. As the filtration process begins, solutes move toward the membrane. Small particles go through the membrane pores and will result in standard blocking. Accumulation of larger particles in the intermediate blocking manner occurs simultaneously. This model is very close to reality and this was verified by the excellent predictions of flux decline due to the combined standard-intermediate blocking model. Combined intermediate blockage-cake formation model also was in good agreement with experimental data and can be applied to separation units where the volume processed decreases in a manner between extremes of cake filtration and intermediate blockage.

2. Modeling

The flow rate can be calculated according to the Darcy's law

$$Q = \frac{dV}{dt} = \frac{PA}{R\mu} \quad (1)$$

Where P is the trans-membrane pressure (Pa), μ is the viscosity of feed solution (Pa.s), A is the membrane area (m²) and R is

the resistance (m^{-1}).

2.1 Intermediate blocking mechanism

In this mechanism it is assumed that membrane consists of parallel pores with constant radius and length, and that each solid particle arriving to the membrane blocks a portion of the pores, and the others superimpose one another. The following equation shows the relationship between available membrane area and volume filtered [11]

$$\frac{A}{A_0} = \exp(-C_{ib}V) \quad (2)$$

In this equation, constant C_{ib} denotes fitted parameter for intermediate blocking model which has units of m^{-1} . The equation can be used both in constant flow rate and constant trans-membrane pressure conditions.

At constant flow rate conditions, Eq. (2) can be written as a function of time [3]

$$\frac{A}{A_0} = \exp(-C_{ib}J_0t) \quad (3)$$

By inserting Eq. (2) into Darcy's law and integrating, the equation of permeate volume as a function of time can be obtained [3]

$$V = \frac{1}{C_{ib}} \ln(1 + C_{ib}J_0t) \quad (4)$$

This equation can then be differentiated to obtain the equation for flux in terms of processing time

$$J = J_0/(1 + C_{ib}J_0t) \quad (5)$$

2.2 Cake filtration mechanism

In cake filtration mechanism it is assumed that particles accumulate on the surface of the membrane and superimpose one upon the other in the form a permeable cake. As the thickness of the cake increases with time so does the resistance to flow. Therefore, the resistance of the cake layer along with the membrane intrinsic resistance contributes to the total resistance. The total resistance increases with volume filtered according to Eq. (6) and with time according to Eq. (7) [3]

$$\frac{R}{R_0} = 1 + C_{cf}J_0V \quad (6)$$

$$\frac{R}{R_0} = \sqrt{1 + 2C_{cf}J_0^2t} \quad (7)$$

where C_{cf} denotes cake filtration constant parameter and has units of $s.m^{-2}$. The volume filtered can be obtained from the following equation [3]

$$V = \frac{1}{C_{cf}J_0} (\sqrt{1 + 2C_{cf}J_0^2t} - 1) \quad (8)$$

This equation can then be differentiated to obtain equation for flux as a function of time

$$J = J_0(1 + 2C_{cf}J_0^2t)^{-0.5} \quad (9)$$

2.3 Standard blocking mechanism

In this mechanism it is assumed that membrane consists of

straight cylindrical pores whose radius decreases with time due to the accumulation of solid particles on the pore walls of the membrane [11, 17]. The following equations show the relationship between resistance and volume filtered (Eq. (10)) or time (Eq. (11)) [3]

$$R = R_0(1 - \frac{C_{sb}V}{2})^{-2} \quad (10)$$

$$R = R_0(1 + \frac{C_{sb}J_0t}{2})^2 \quad (11)$$

In these equations, constant C_{sb} denotes fitted parameter for standard blocking model which has units of m^{-1} . The equation of permeate volume as a function of time thus can be obtained [3]

$$V = (\frac{1}{J_0t} + \frac{C_{sb}}{2})^{-1} \quad (12)$$

By differentiating the above equation, the equation of flux can be obtained as follows

$$J = \frac{1}{J_0t^2} (\frac{1}{J_0t} + \frac{C_{sb}}{2})^{-2} \quad (13)$$

2.4 Combined cake filtration-intermediate blocking model

Bolton et al. developed a combined model accounting for the effects of intermediate blockage and cake formation mechanisms. Filtration area loss predicted by the intermediate blocking mechanism was combined with the resistance from caking. Equation for volume filtered as a function of time can be obtained by inserting Eq. (2) and Eq. (7) into Darcy's equation [3]

$$V = \frac{1}{C_{ib}} \ln(1 + \frac{C_{ib}}{C_{cf}J_0} ((1 + 2C_{cf}J_0^2t)^{0.5} - 1)) \quad (14)$$

The equation can then be differentiated to obtain the equation for flux in terms of time

$$J = J_0(1 + 2C_{cf}J_0^2t)^{-0.5} / (1 + \frac{C_{ib}}{C_{cf}J_0} ((1 + 2C_{cf}J_0^2t)^{0.5} - 1)) \quad (15)$$

In case of caking, the equation of resistance R versus time, Eq. (7), was used. The equation of R as a function of V cannot be used, since volume filtered is defined relative to the available membrane area, which is decreasing during the experiment.

In case of intermediate blocking, equation of area in terms of volume filtered was used. The equation of area loss as a function of time is not valid here, since the rate of intermediate blocking with respect to time is slower than cake formation. A detailed description of these models is provided by Bolton et al. [3].

2.5 Combined standard-intermediate blocking model

Bolton et al. developed a combined model accounting for the effects of intermediate blockage and standard blocking

mechanisms using a similar technique. Filtration area loss predicted by the intermediate blocking mechanism was combined with the resistance due to pore destruction. Equation for volume filtered as a function of time can be obtained by inserting Eq. (2) and Eq. (11) into Darcy's equation [3]

$$V = \frac{1}{C_{ib}} \ln\left(1 + \frac{2C_{ib}J_0t}{2 + C_{sb}J_0t}\right) \quad (16)$$

The equation can then be differentiated to obtain the equation for flux in terms of time

$$J = \frac{2}{C_{ib}t(2 + C_{sb}J_0t)} \quad (17)$$

A summary of these models is provided in Table 1.

3. Experimental

3.1 Skim milk ultrafiltration using a spiral wound module

The experimental data used in this paper were obtained from previous studies of skim milk ultrafiltration done by Razavi et al. [10]. They used a spiral wound membrane ultrafiltration unit (Biocon Company, Moscow, Russia). The membrane material was polysulfone amide with a 20-kDa molecular weight cut off.

The membrane system was equipped to a tubular heat exchanger and a temperature sensor to keep the feed at constant temperature of 40 °C. Membrane unit was also installed to a feed tank (20 L) and a flow meter measured the feed flow rate which was constant at 15 L.min⁻¹ [10].

The membrane module was 0.47 m in length with 0.11 m inner radius, providing membrane surface area of 0.33 m².

Two pressure gauges measured inlet pressure (P_{in}) and outlet pressure (P_{out}). The TMP was obtained by the following equation [10]

$$TMP = \frac{1}{2}(P_{in} + P_{out}) - P_{permeate} \quad (18)$$

Feed solution was prepared by mixing skim milk powder with water at a temperature of about 50 °C in a blender, providing final pH of 6.54. Average content of total solid (TS) and water in produced solution was 8.443 and 91.557 %, respectively. Experiments were carried out at different TMPs (50, 100, 150, 200 and 250 kPa) to investigate the effect of pressure on flux decline. All experimental runs repeated twice. For each filtration run, the water was first contacted with membrane to measure water flux. Membrane intrinsic resistance then was calculated according to Darcy's law [10]

$$R_{i,m} = \frac{TMP}{\mu_{permeate} J_{permeate}} \quad (19)$$

Where $\mu_{permeate}$ denotes permeate dynamic viscosity (water dynamic viscosity) (Pa.s) and $R_{i,m}$ denotes membrane intrinsic resistance (m⁻¹). Then the water was replaced with reconstituted skim milk at 40 °C. The permeate flux was measured and recorded every 30 s.

After 30 min filtration, the operation was stopped and the membrane system was cleaned by distilled water and NaOH

solution according to the protocol described by manufacturer.

3.2 Skim milk ultrafiltration using a Pellicon cassette module

Rinaldoni et al. used a Pellicon cassette membrane ultrafiltration unit (Millipore, USA) [18]. The membrane material was modified polysulfone with a 10-kDa molecular weight cut off and total membrane surface area of 0.5 m².

The feed solution was partially skimmed milk supplied by MILKAUT which was first heated in a water bath. The feed solution then was pumped through the membrane system with a constant feed flow rate of 29 ± 0.05 L.min⁻¹.

The effect of different pressures (0.5, 1 and 1.5 bar) and different temperatures (20, 30 and 40 °C) on flux was investigated. All experiments were carried out twice.

4. Results

4.1 Skim milk concentration with spiral wound ultrafiltration module

The combined cake filtration-intermediate blocking model was compared with combined standard-intermediate blocking model and experimental data for the concentration of reconstituted skim milk. Experiments were performed using a polysulfone amide ultrafiltration membrane with twelve kilograms of reconstituted skim milk at constant temperature and flow rate (40 °C and 15 L.min⁻¹, respectively) [10]. To investigate the effect of pressure on flux decline, experiments were carried out at 50, 100, 150, 200 and 250 kPa trans-membrane pressures. The permeate flux was measured as a function of time and recorded every 30 s.

The data and the model predictions for skim milk samples at different pressures are shown in Fig. 1. Applying cake formation mechanism simultaneously with intermediate blocking mechanism (solid green lines) resulted in a very good data fit. However, combined intermediate-standard blocking model (dashed red lines) better fitted the empirical data with error values considerably lower than combined cake formation-intermediate blocking model, as it can be seen in Table 2. Lowest error value of combined cake formation-intermediate blocking model were 5.35 × 10⁻¹ and 5.68 × 10⁻¹ obtained at 250 and 50 kPa TMP, respectively. Lowest standard error values of combined standard-intermediate blocking model were 2.97 × 10⁻¹ and 4.12 × 10⁻¹ obtained at 50 and 250 kPa TMP, respectively. Thus combined standard-intermediate blocking model can be applied effectively for separation systems where volume filtered decreases in a manner between the extremes of standard blocking and intermediate blockage.

The calculated fitted parameters versus iteration using Curve Expert are shown in Fig. 2. As it can be seen in Fig. 2(a), the number of iterations used for calculating C_{cb} in combined cake filtration-intermediate blocking model (red solid line) was more than 10 at pressures more than 50 kPa and 0 at 50kPa, while it was 0 for calculating C_{ib} (green solid lines) at all

pressures. This means that Curve Expert is converged after more than 10 iterations for C_{cb} at high and moderate pressures, while converged without any iteration for C_{cb} at 50 kPa and for C_{ib} at all pressures.

Fig. 3 shows the effect of different trans-membrane pressures on flux. Averaged values of flux were used and the data was modeled using Power regression (solid blue lines) and Modified Exponential regression (solid red lines). For Power regression, the following equation was used

$$Y = ax^b \quad (20)$$

For Modified Exponential regression, the following equation was used

$$Y = ae^{b/x} \quad (21)$$

in which a and b are constant parameters, which are obtained by regression and their values are shown in Table 3. As it can be seen from Fig. 3, flux increased by increasing TMP. Power regression was in excellent agreement with actual values (blue solid circles), with error value approximately half the Modified Exponential regression.

4.2 Skim milk concentration with Pellicon cassette ultrafiltration module

Experiments were performed using a modified polysulfone ultrafiltration membrane with partially skimmed milk at constant flow rate ($29 \pm 0.05 \text{ L}\cdot\text{min}^{-1}$) [18]. To investigate the effect of pressure on flux decline, experiments were carried out at 0.5, 1 and 1.5 bar trans-membrane pressures. Fig. 4 shows the effect of different pressures on flux decline. As it can be seen from the figure, predictions of combined standard-intermediate blocking model (dashed red lines) were in excellent agreement with experimental data and that's error values were considerably lower than combined cake formation-intermediate blocking model. Standard error values of these models are provided in Table. 4.

To investigate the effect of temperatures on flux decline, experiments were carried out at 20, 30 and 40 °C. Fig. 5 shows the effect of different temperatures on flux decline. With increasing temperature, the flux data were increased slightly. Similar to the data for flux versus pressure, predictions of combined standard-intermediate blocking model (Fig. 5(b)) were in excellent agreement with experimental data and that's error values were considerably lower than combined cake formation-intermediate blocking model, as it can be seen from Table. 5.

The calculated fitted parameters versus iteration using Curve Expert are shown in Fig. 6. As it can be seen in Fig. 6(a,b), the number of iterations used for calculating fitted parameters in combined cake filtration-intermediate blocking model and combined intermediate-standard blocking model at different TMPs were less than 5 and 6, respectively. This means that fitted parameters of combined cake formation-intermediate blocking model and combined intermediate-standard blocking model did not changed after approximately 5 and 6 iterations, respectively, and that Curve Expert converged at this values.

The effect of different trans-membrane pressures and temperatures on flux decline is shown in Fig. 7 and Fig. 8, respectively. Averaged values of flux were used and the data of flux versus TMP and temperature was modeled using Exponential regression (solid blue line) and Reciprocal Logarithm regression (red solid line). For Exponential regression, the following equation was used

$$Y = ae^{bx} \quad (22)$$

For Reciprocal Logarithm regression, the following equation was used

$$Y = \frac{1}{a + b \ln x} \quad (23)$$

As it can be seen from Fig. 7 and Fig. 8, flux increased by increasing both TMP and temperature. Error values of two regressions are shown in Table 6 (flux vs. TMP) and Table 7 (flux vs. temperature). Reciprocal Logarithm regression was better fitted the data sets of flux versus TMP, while predictions of Exponential regression were better for flux data versus temperature.

5. Conclusions

To simulate fouling in milk concentration process, combined cake filtration-intermediate blocking model proposed by Bolton et al. was applied and compared to combined standard-intermediate blocking model and data for skim milk at constant flow operation. The combined models used two fitted parameters and simplified to the equations for the typical mechanisms when the effects of second fouling mechanism were negligible.

The applicability of model to data for the skim milk concentration at different trans-membrane pressures and temperatures was tested. The combined standard-intermediate blocking model provided the best fit of the data sets and was in excellent agreement with experimental results. Thus, combined standard-intermediate blocking model can be regarded as an effective model for predicting flux decline in solutions where the volume filtered decreases in a manner between the extremes of standard and intermediate blocking. The combined intermediate blocking-cake formation model also provided good simulations and can be applied to solutions where the volume filtered decreases in a manner between the extremes of cake formation and intermediate blocking.

Nomenclature

A	available membrane area (m ²)
A ₀	initial membrane area (m ²)
a	regression constant parameter
b	regression constant parameter
C _{ib}	intermediate blocking constant (m ⁻¹)
C _{cf}	cake filtration constant (s.m ⁻²)
J	flux (m.s ⁻¹)
J ₀	initial flux (m.s ⁻¹)
J _{permeate}	permeate flux (m.s ⁻¹)
P _{in}	inlet pressure (Pa)
P _{out}	outlet pressure (Pa)

P_{permeate}	permeate pressure (Pa)
Q	flow rate ($\text{m}^3 \cdot \text{s}^{-1}$)
R	resistance to flow (m^{-1})
R_0	initial resistance to flow (m^{-1})
$R_{i,m}$	intrinsic membrane resistance (m^{-1})
t	time (s)
TMP	trans-membrane pressure (Pa)
V	volume filtered ($\text{m}^3 \cdot \text{m}^{-2}$)
μ	feed viscosity ($\text{kg} \cdot \text{m}^{-1} \cdot \text{s}^{-1}$)
μ_{permeate}	permeate dynamic viscosity ($\text{kg} \cdot \text{m}^{-1} \cdot \text{s}^{-1}$)

References

- [1] A. Mirzaei, T. Mohammadi, Effect of ultrasonic waves on flux enhancement in microfiltration of milk, *Journal of Food Engineering*, 108, 77-86, 2012.
- [2] M. Taghipour, Review of cleaning methods of ultrafiltration membranes in milk industries, Ms. Thesis, Iran University of Science & Technology, Iran, 1999.
- [3] G. Bolton, D. LaCasse, R. Kuriyel, Combined models of membrane fouling: development and application to microfiltration and ultrafiltration of biological fluids, *Journal of Membrane Science*, 277, 75-84, 2006.
- [4] P. Aimar, S. Baklouti, V. Sanchez, Membrane-solute interactions: influence on pure solvent transfer during ultrafiltration, *Journal of Membrane Science*, 29, 207-224, 1986.
- [5] J. L. Maubois, Ultrafiltration of whey, *Journal of the Society of Dairy Technology*, 33, 55-58, 1980.
- [6] A. Guadix, J. E. Zapata, M. C. Almecija, E. M. Guadix, Predicting the flux decline in milk cross-flow ceramic ultrafiltration by artificial neural network, *Desalination*, 250, 1118-1120, 2010.
- [7] X. T. Jimenez, A. A. Cuenca, A. T. Jurado, A. A. Corona, C. R. M. Urista, Traditional methods for whey protein isolation and concentration: effects on nutritional properties and biological activity, *Journal of the Mexican Chemical Society*, 56, 369-377, 2012.
- [8] H. Rezaei, F. Z. Ashtiani, A. Fouladitajar, Fouling behavior and performance of microfiltration membranes for whey treatment in steady and unsteady-state conditions, *Brazilian Journal of Chemical Engineering*, 31, 503-518, 2014.
- [9] M. Kazemimoghaddam, T. Mohammadi, Chemical cleaning of ultrafiltration membranes in milk industry, *Desalination*, 204, 213-218, 2007.
- [10] M. A. Razavi, A. Mortazavi, M. Mousavi, Dynamic modeling of milk ultrafiltration by artificial neural network, *Journal of Membrane Science*, 220, 47-58, 2003.
- [11] J. Hermia, Constant pressure blocking filtration laws: application to power-law non-Newtonian fluids, *Chemical Engineering Research and Design*, 60, 183-187, 1982.
- [12] K. Katsoufidou, S. G. Yiantsios, A. J. Karabelas, A study of ultrafiltration membrane fouling by humic acids and flux recovery by backwashing: experiments and modeling, *Journal of Membrane Science*, 266, 40-50, 2005.
- [13] S. Mattaraj, C. Jarusutthirak, C. Charoensuk, R. Jiraratananon, A combined pore blockage, osmotic pressure and cake filtration model for crossflow nanofiltration of natural organic matter and inorganic salts, *Desalination*, 274, 182-191, 2011.
- [14] M-J. Corbaton-Baguena, M-C. Vincent-Vela, S. Alvarez Blanco, J. Lora-Garcia, Analysis of two ultrafiltration fouling models and estimation of model parameters as a function of operational conditions, *Transport in Porous Media*, 99, 391-411, 2013.
- [15] V. B. Briao, C. R. G. Tavares, Pore blocking mechanism for the recovery of milk solids from dairy wastewaters by ultrafiltration, *Brazilian Journal of Chemical Engineering*, 29, 93-407, 2012.
- [16] C-C. Ho, A. L. Zydney, Trans-membrane pressure profiles during constant flux microfiltration of bovine serum albumin, *Journal of Membrane Science*, 209, 363-377, 2002.
- [17] H. P. Grace, Structure and performance of filter media, *AIChE Journal*, 2, 307, 1956.
- [18] A. N. Rinaldoni, C. C. Tarazaga, M. E. Campderros, A. P. Padilla, Assessing performance of skim milk ultrafiltration by using technical parameters, *Journal of Food Engineering*, 92, 226-232, 2009.

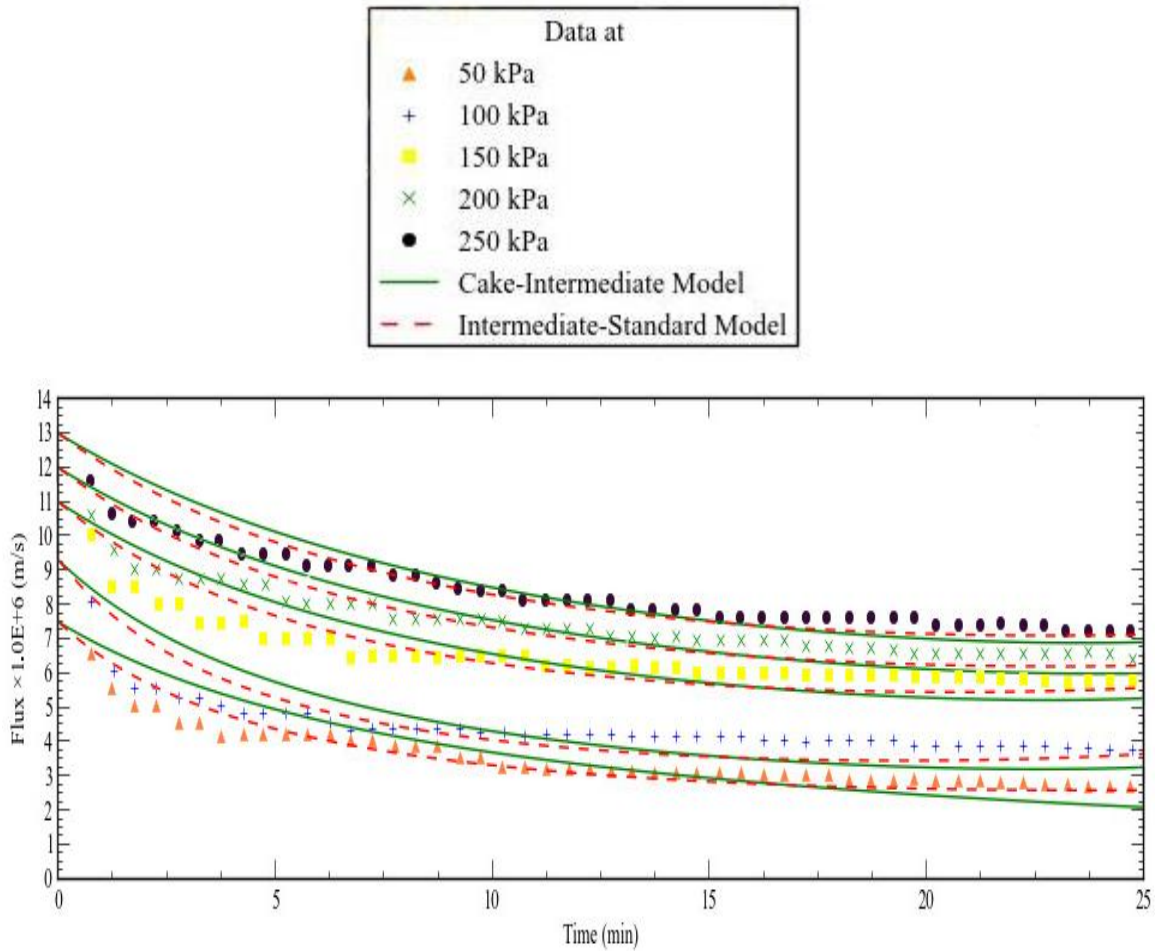
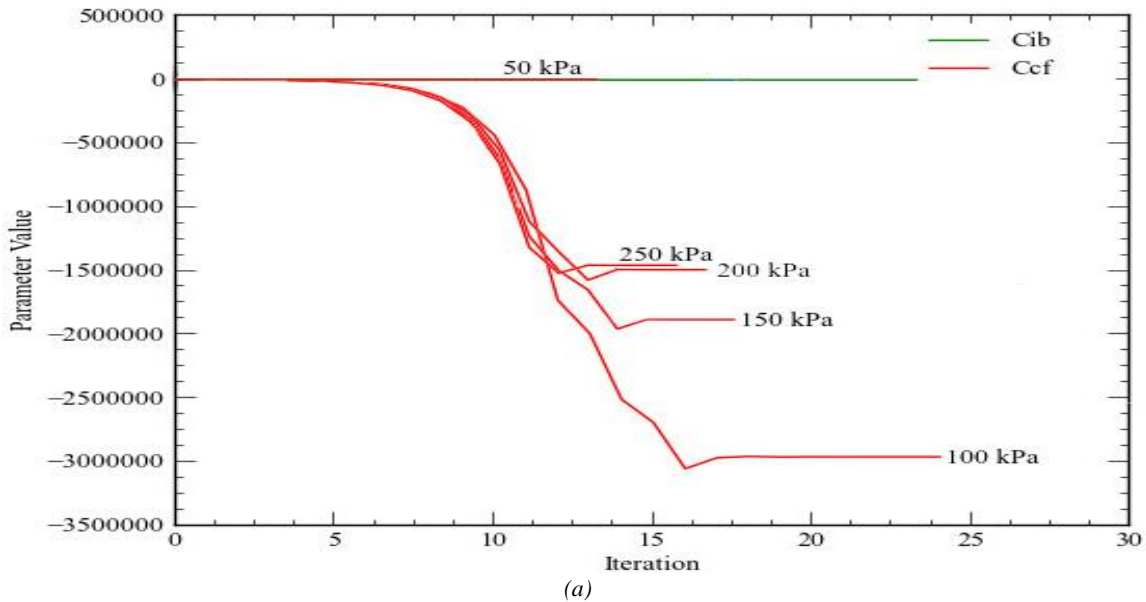


Figure 1: Flux vs. time data for skim milk through spiral wound ultrafiltration membrane module compared to the combined cake formation-intermediate blocking model and combined standard-intermediate blocking model



(a)

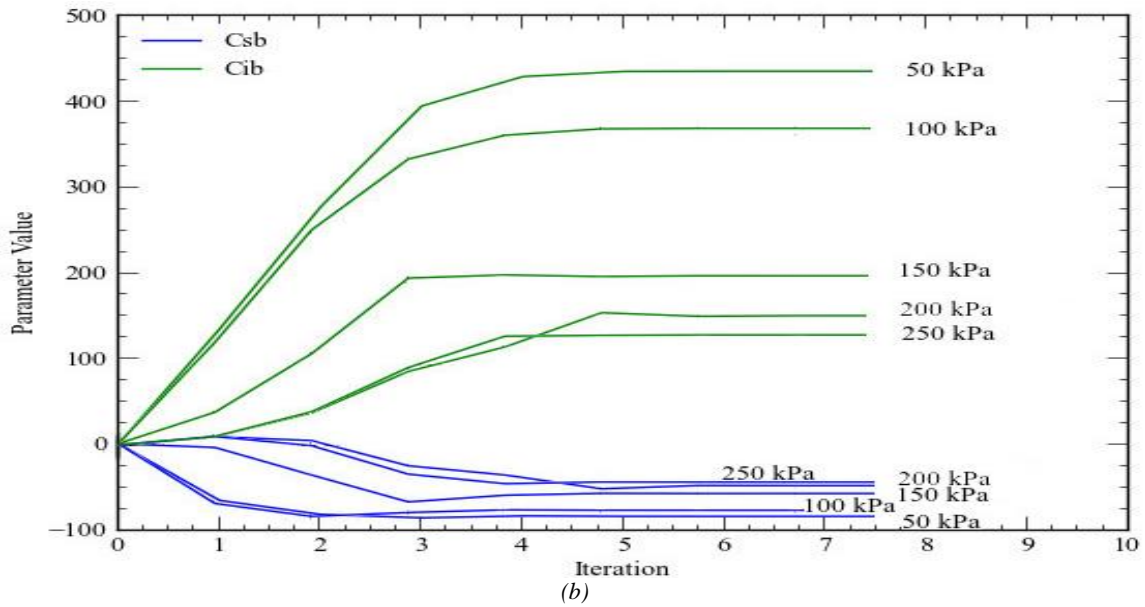


Figure 2: Calculated fitted parameters vs. iteration by Curve Expert: (a) combined cake filtration-intermediate blocking flux prediction and (b) combined standard-intermediate flux prediction

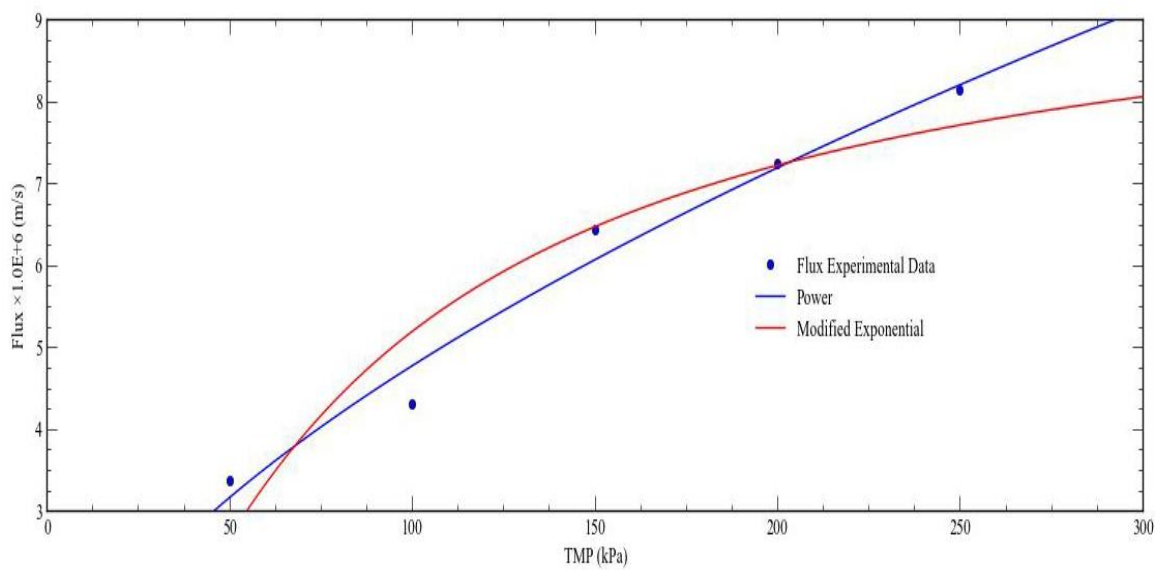
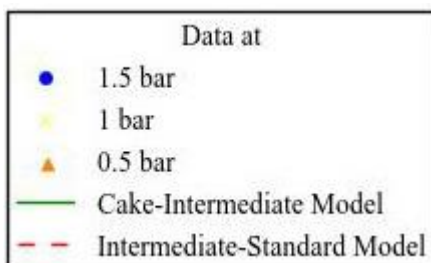


Figure 3: Averaged data values of flux vs. TMP for skim milk through spiral wound ultrafiltration membrane module compared to the Power and Modified Exponential regressions



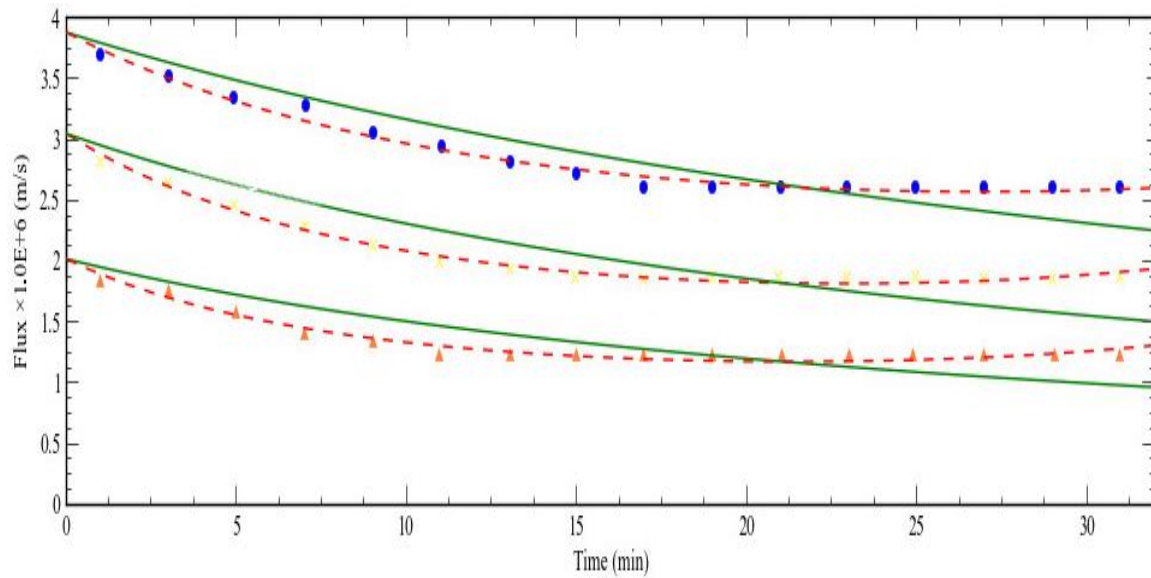
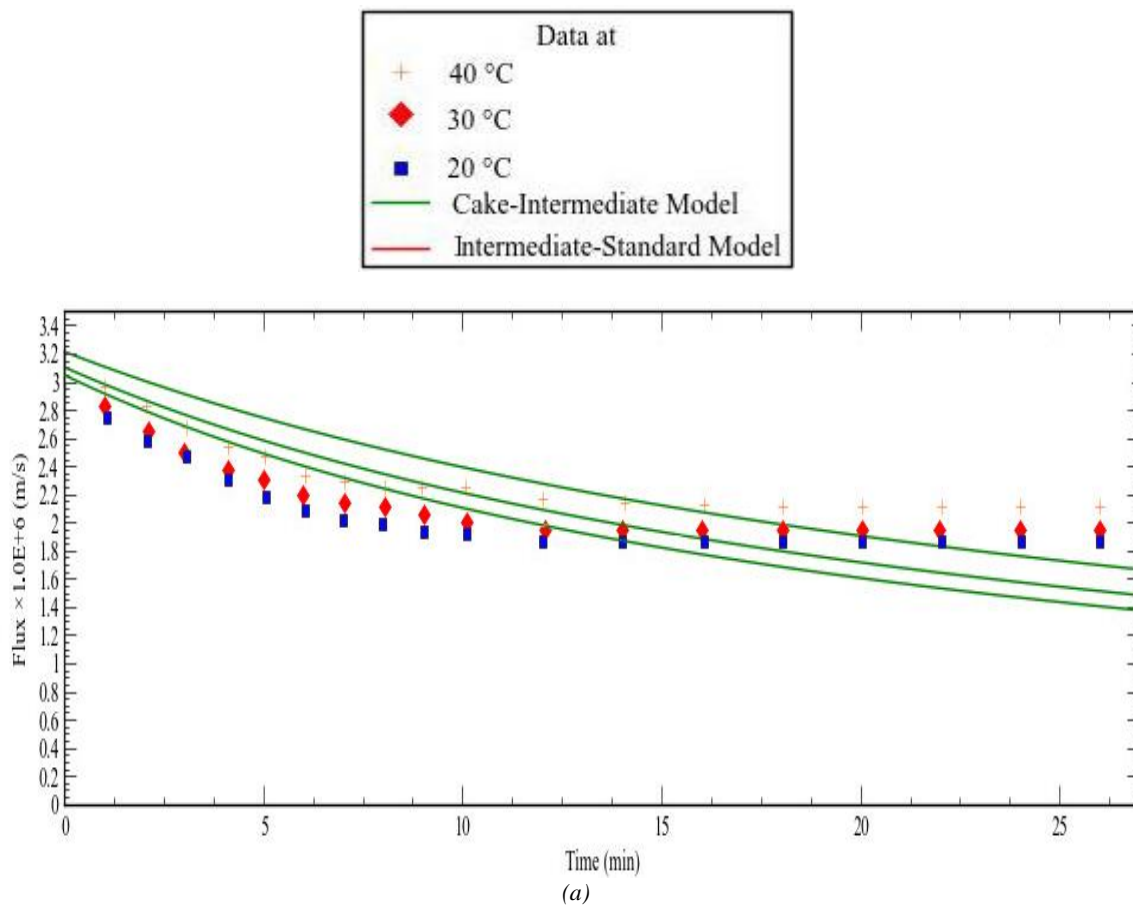


Figure 4: Flux vs. time data for partially skimmed milk through Pellicon cassette ultrafiltration membrane module compared to the combined cake formation-intermediate blocking model and combined standard-intermediate blocking model at different pressures



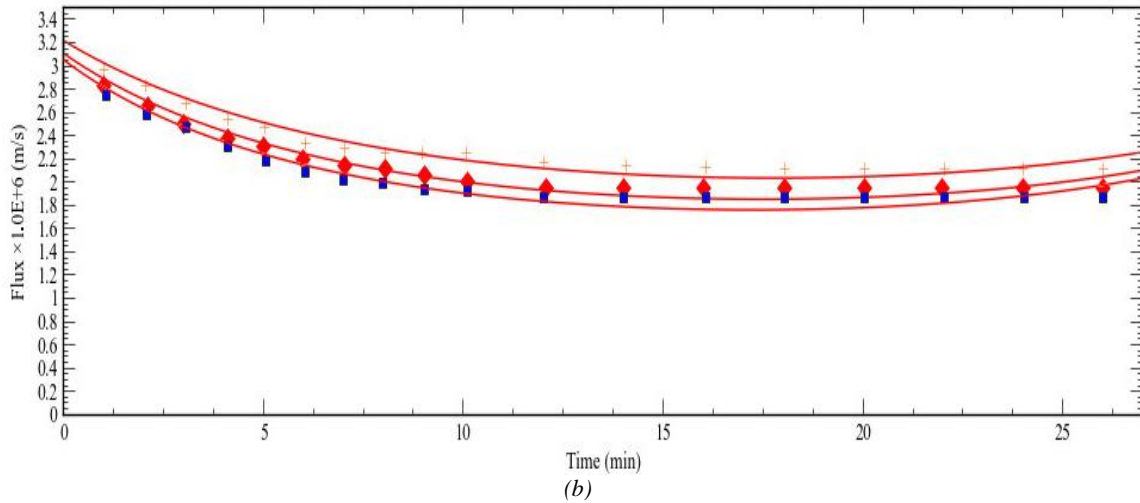
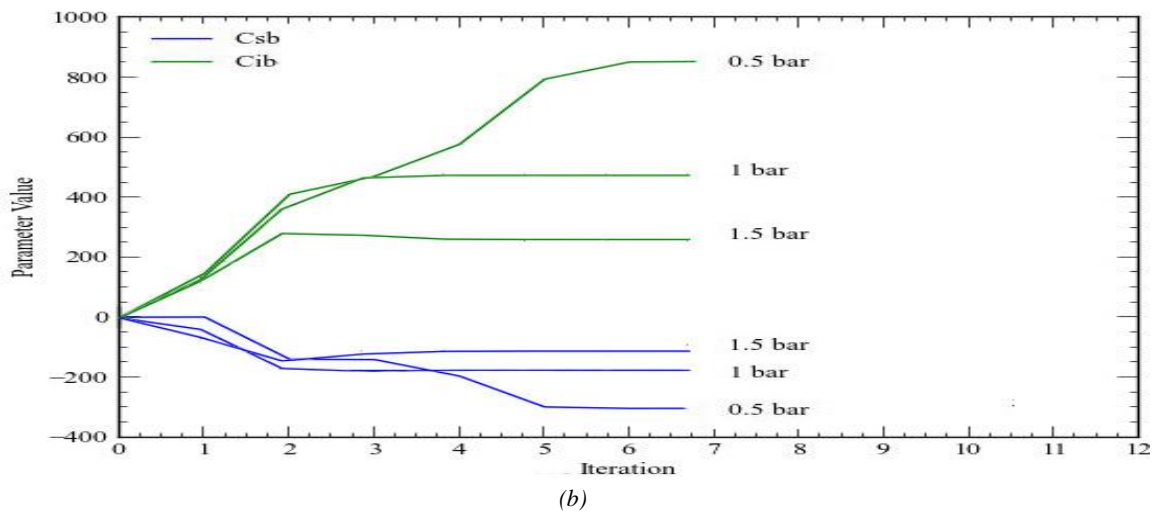
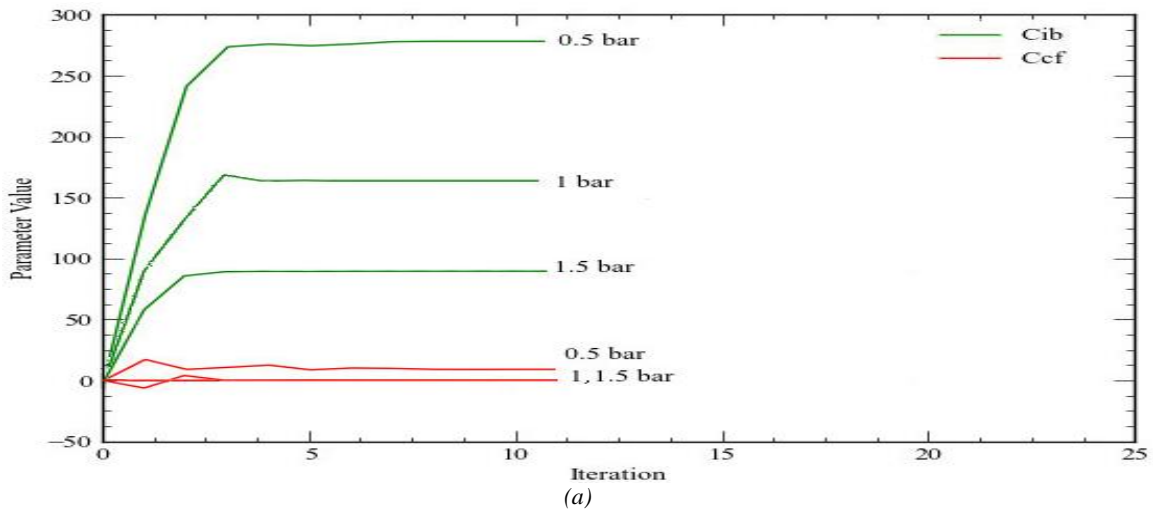


Figure 5: Flux vs. time data for partially skimmed milk through Pellicon cassette ultrafiltration membrane module compared to the (a) combined cake formation-intermediate blocking model and (b) combined standard-intermediate blocking model at different temperatures



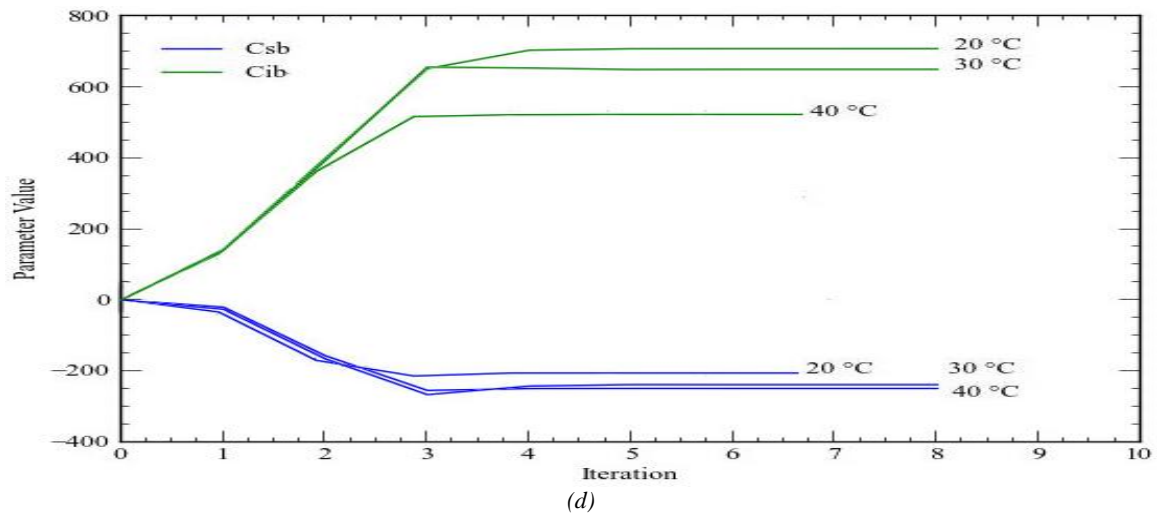
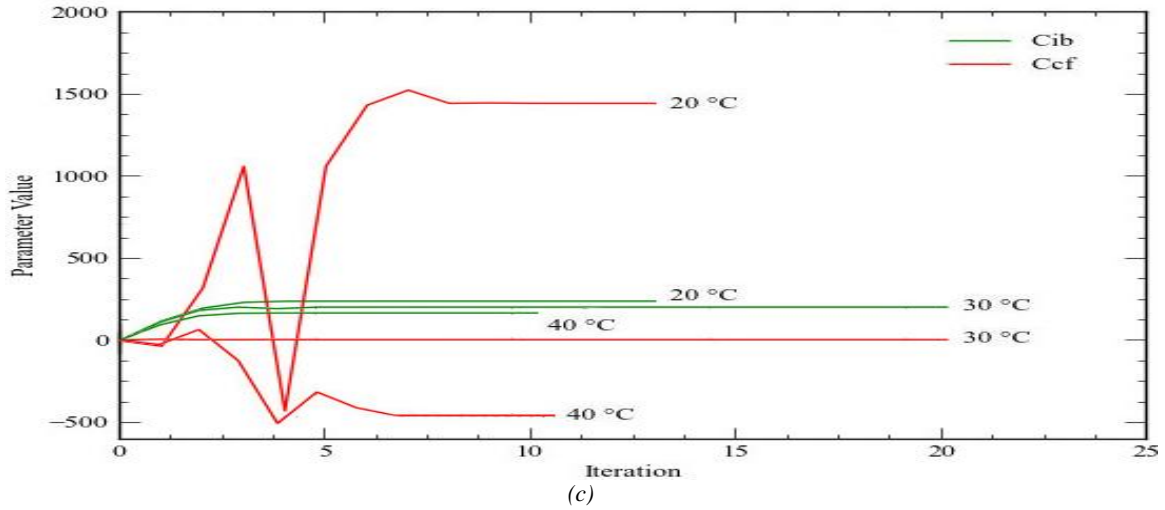


Figure 6: Calculated fitted parameters of combined cake filtration-intermediate blocking model vs. iteration by Curve Expert at different pressures (a) and different temperatures (c), and fitted parameters of combined standard-intermediate blocking model at different pressures (b) and different temperatures (d)

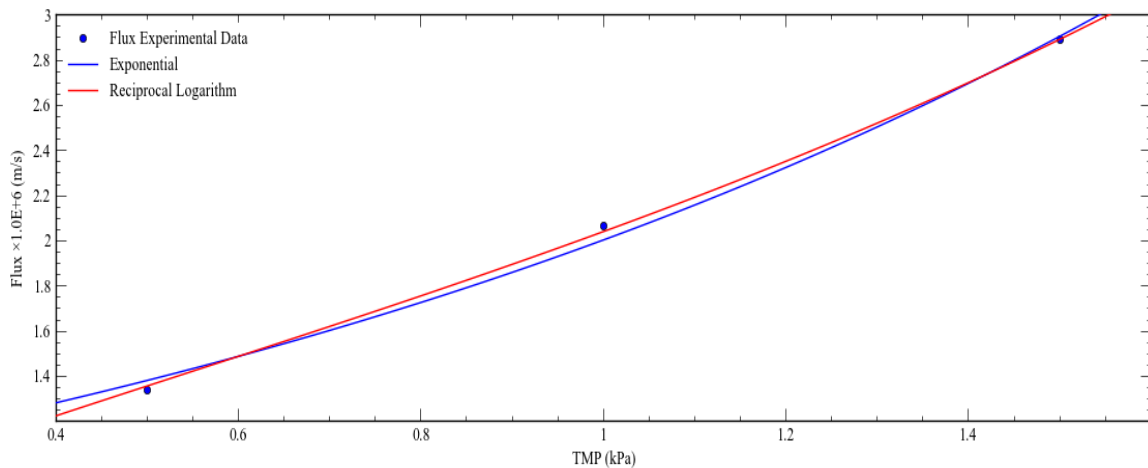


Figure 7: Averaged data values of flux vs. TMP for partially skimmed milk through Pellicon cassette ultrafiltration membrane module compared to the Reciprocal Logarithm and Exponential regressions

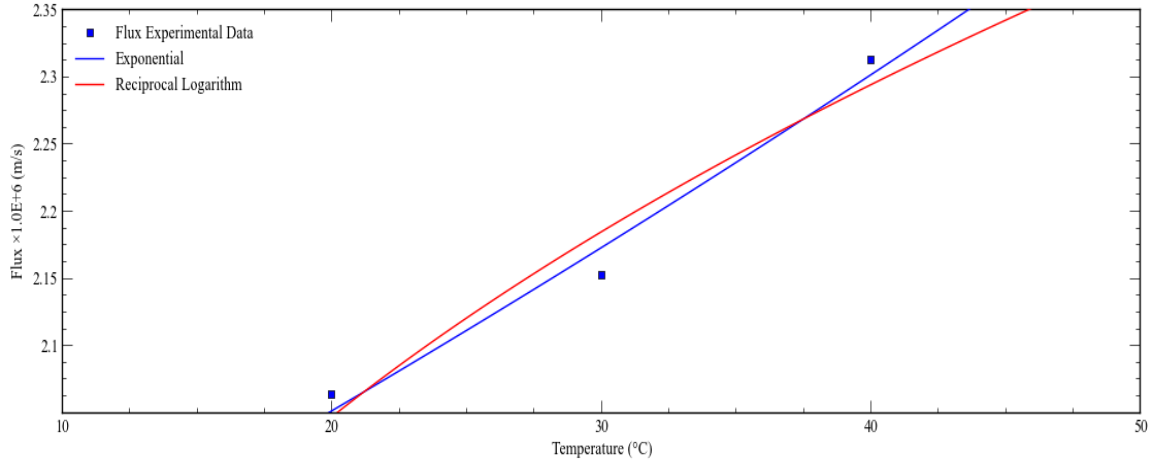


Figure 8: Averaged data values of flux vs. temperature for partially skimmed milk through Pellicon cassette ultrafiltration membrane module compared to the Reciprocal Logarithm and Exponential regressions

Table 1: Summary of the flux equations for cake filtration model, intermediate blocking model, standard blocking model, combined standard-intermediate blocking model and combined cake formation-intermediate blocking model

Model	Equation	Fitted parameters
Cake filtration (Eq. (9))	$J = J_0(1 + 2C_{cf}J_0^2t)^{-0.5}$	C_{cf} (s.m ⁻²)
Intermediate blocking (Eq. (5))	$J = J_0/(1 + C_{ib}J_0t)$	C_{ib} (m ⁻¹)
Standard blocking (Eq. (13))	$J = \frac{1}{J_0t^2} \left(\frac{1}{J_0t} + \frac{C_{sb}}{2} \right)^{-2}$	C_{sb} (m ⁻¹)
Cake-intermediate (Eq. (15))	$J = J_0(1 + 2C_{cf}J_0^2t)^{-0.5} / \left(1 + \frac{C_{ib}}{C_{cf}J_0} \left((1 + 2C_{cf}J_0^2t)^{0.5} - 1 \right) \right)$	C_{cf} (s.m ⁻²), C_{ib} (m ⁻¹)
Standard-intermediate (Eq. (17))	$J = \frac{2}{C_{ib}t(2 + C_{sb}J_0t)}$	C_{sb} (m ⁻¹), C_{ib} (m ⁻¹)

Table 2: Combined cake filtration-intermediate blocking model and combined intermediate-standard blocking model standard error values and fitted parameters for skim milk ultrafiltration through spiral wound membrane module at different TMPs

Model	Model standard error	Fit parameter values
Cake-intermediate (Eq. (15))	5.68×10^{-1}	$C_{ib} = 2.28 \times 10^2$ m ⁻¹ (50 kPa), $C_{cf} = -3.86 \times 10^1$ s.m ⁻² (50 kPa)
	7.5×10^{-1}	$C_{ib} = 2.60 \times 10^2$ m ⁻¹ (100 kPa), $C_{cf} = -2.96 \times 10^6$ s.m ⁻² (100 kPa)
	6.53×10^{-1}	$C_{ib} = 1.38 \times 10^2$ m ⁻¹ (150 kPa), $C_{cf} = -2.00 \times 10^6$ s.m ⁻² (150 kPa)
	6.30×10^{-1}	$C_{ib} = 1.11 \times 10^2$ m ⁻¹ (200 kPa), $C_{cf} = -1.58 \times 10^6$ s.m ⁻² (200 kPa)
	5.35×10^{-1}	$C_{ib} = 9.42 \times 10^1$ m ⁻¹ (250 kPa), $C_{cf} = -1.35 \times 10^6$ s.m ⁻² (250 kPa)
Intermediate-standard (Eq. (17))	2.97×10^{-1}	$C_{ib} = 4.36 \times 10^2$ m ⁻¹ (50 kPa) $C_{sb} = -8.36 \times 10^1$ m ⁻¹ (50 kPa)
	5.56×10^{-1}	$C_{ib} = 3.92 \times 10^2$ m ⁻¹ (100 kPa) $C_{sb} = -8.16 \times 10^1$ m ⁻¹ (100 kPa)
	4.8×10^{-1}	$C_{ib} = 2.09 \times 10^2$ m ⁻¹ (150 kPa) $C_{sb} = -6.09 \times 10^1$ m ⁻¹ (150 kPa)
	5.09×10^{-1}	$C_{ib} = 1.62 \times 10^2$ m ⁻¹ (200 kPa) $C_{sb} = -4.94 \times 10^1$ m ⁻¹ (200 kPa)
	4.12×10^{-1}	$C_{ib} = 1.38 \times 10^2$ m ⁻¹ (250 kPa) $C_{sb} = -4.5 \times 10^1$ m ⁻¹ (250 kPa)

Table 3: Power and Modified Exponential regression standard error values and constant parameters for skim milk ultrafiltration through spiral wound membrane module at different TMPs

Regression	Regression standard error	a	b
Power	3.62×10^{-1}	3.19×10^{-1}	5.89×10^{-1}
Modified exponential	6.92×10^{-1}	1.00×10^1	-6.56×10^1

Table 4: Combined cake filtration-intermediate blocking model and combined intermediate-standard blocking model standard error values and fitted parameters for partially skimmed milk ultrafiltration through Pellicon cassette membrane module at different TMPs

Model	Model standard error	Fit parameter values
Cake-intermediate (Eq. (15))	1.71×10^{-1}	$C_{ib} = 2.79 \times 10^2 \text{ m}^{-1}$ (0.5 bar), $C_{cf} = 9.91 \text{ s.m}^{-2}$ (0.5 bar)
	2.12×10^{-1}	$C_{ib} = 1.74 \times 10^2 \text{ m}^{-1}$ (1 bar), $C_{cf} = -2.74 \times 10^{-1} \text{ s.m}^{-2}$ (1 bar)
	1.79×10^{-1}	$C_{ib} = 9.66 \times 10^1 \text{ m}^{-1}$ (1.5 bar), $C_{cf} = 1.48 \text{ s.m}^{-2}$ (1.5 bar)
Intermediate-standard (Eq. (17))	0.47×10^{-1}	$C_{ib} = 8.54 \times 10^2 \text{ m}^{-1}$ (0.5 bar) $C_{sb} = -3.03 \times 10^2 \text{ m}^{-1}$ (0.5 bar)
	0.39×10^{-1}	$C_{ib} = 5.07 \times 10^2 \text{ m}^{-1}$ (1 bar) $C_{sb} = -1.85 \times 10^2 \text{ m}^{-1}$ (1 bar)
	0.51×10^{-1}	$C_{ib} = 2.79 \times 10^2 \text{ m}^{-1}$ (1.5 bar) $C_{sb} = -1.17 \times 10^2 \text{ m}^{-1}$ (1.5 bar)

Table 5: Combined cake filtration-intermediate blocking model and combined intermediate-standard blocking model standard error values and fitted parameters for partially skimmed milk ultrafiltration through Pellicon cassette membrane module at different temperatures

Model	Model standard error	Fit parameter values
Cake-intermediate (Eq. (15))	2.81×10^{-1}	$C_{ib} = 2.43 \times 10^2 \text{ m}^{-1}$ (20 °C), $C_{cf} = 1.45 \times 10^3 \text{ s.m}^{-2}$ (20 °C)
	2.68×10^{-1}	$C_{ib} = 2.14 \times 10^2 \text{ m}^{-1}$ (30 °C), $C_{cf} = 2.84 \text{ s.m}^{-2}$ (30 °C)
	2.56×10^{-1}	$C_{ib} = 1.76 \times 10^2 \text{ m}^{-1}$ (40 °C), $C_{cf} = -4.89 \times 10^2 \text{ s.m}^{-2}$ (40 °C)
Intermediate-standard (Eq. (17))	0.65×10^{-1}	$C_{ib} = 7.09 \times 10^2 \text{ m}^{-1}$ (20 °C) $C_{sb} = -2.49 \times 10^2 \text{ m}^{-1}$ (20 °C)
	0.58×10^{-1}	$C_{ib} = 6.51 \times 10^2 \text{ m}^{-1}$ (30 °C) $C_{sb} = -2.38 \times 10^2 \text{ m}^{-1}$ (30 °C)
	0.63×10^{-1}	$C_{ib} = 5.56 \times 10^2 \text{ m}^{-1}$ (40 °C) $C_{sb} = -2.2 \times 10^2 \text{ m}^{-1}$ (40 °C)

Table 6: Reciprocal Logarithm and Exponential regression standard error values and constant parameters for partially skimmed milk ultrafiltration through Pellicon cassette membrane module at different TMPs

Regression	Regression standard error	a	b
Exponential	0.77×10^{-1}	9.56×10^{-1}	7.42×10^{-1}
Reciprocal Logarithm	0.31×10^{-1}	4.89×10^{-1}	-3.54×10^{-1}

Table 7: Reciprocal Logarithm and Exponential regression standard error values and constant parameters for partially skimmed milk ultrafiltration through Pellicon cassette membrane module at different temperatures

Regression	Regression standard error	a	b
Exponential	0.26×10^{-1}	1.83	5.75×10^{-3}
Reciprocal Logarithm	0.4×10^{-1}	7.16×10^{-1}	-7.58×10^{-2}